Performance of Star 16/64QAM Schemes Using Turbo FDE with Iterative Decision-Directed Channel Estimation for DFT-Precoded OFDMA

Chihiro Mori[1], Mamoru Sawahash[1], Teruo Kawamura[2], and Nobuhiko Miki[3]

[1]Tokyo City University, Tokyo, Japan
[2]NTT Docomo INC., Yokosuka, Japan
[3]Kagawa University, Takamatsu, Japan
Email: mori@mobile.cn.tcu.ac.jp; sawahasi@tcu.ac.jp, kawamurate@nttdocomo.com, miki@eng.kagawa-u.ac.jp

Abstract—This paper presents the average block error rate (BLER) performance of star 16/64QAM schemes using iterative decision-directed channel estimation (IDDCE) associated with the turbo frequency domain equalizer (FDE) for discrete Fourier transform (DFT)-precoded Orthogonal Frequency Division Multiple Access (OFDMA). We show that the turbo FDE with the IDDCE based on the *a posteriori* log-likelihood ratio (LLR) decreases the required average received signal-to-noise power ratio (SNR) compared to that based on the extrinsic LLR. We also show that the turbo FDE is effective in decreasing the required average received SNR considering the cubic metric (CM) compared to the linear minimum mean-square error based FF-FDE for star 16/64QAM schemes. Moreover, we show that the (8, 8) star 16QAM and (16, 16, 16, 16) star 64QAM schemes decrease the required average received SNR considering the CM at the average BLER of 10^{-2} by approximately 0.8 and 0.3 dB compared to the square 16QAM and 64QAM schemes, respectively, with a low turbo coding rate such as $R = 1/3$ when using the turbo FDE associated with IDDCE.

Index Terms—single-carrier FDMA; turbo FDE; iterative channel estimation; star QAM; DFT-precoded OFDMA

I. INTRODUCTION

Single-carrier (SC)-Frequency Division Multiple Access (FDMA) is adopted in the Long-Term Evolution (LTE) uplink due to its low peak-to-average power ratio (PAPR) feature [1]. Discrete Fourier transform (DFT)-precoded Orthogonal Frequency Division Multiple Access (OFDMA) is adopted to generate SC-FDMA signals in the frequency domain [2], [3] to achieve high commonality with OFDMA in the downlink and affinity to frequency domain equalizers (FDEs) [4], [5].

In adaptive modulation and coding (AMC), high-level modulation schemes including 16QAM and 64QAM are employed near a cell site under high-received signal-to-interference plus noise power ratio (SINR) conditions. Square 16/64QAM schemes are usually employed because they have the longest Euclidean distances among constellation signals [6]. Recently, the star 16QAM scheme [7] has drawn attention due to its merit, i.e., the fluctuation in amplitude is smaller than that for the square

16QAM scheme. It was clarified in [8] that the (8, 8) star 16QAM scheme achieves a lower required average received signal-to-noise power ratio (SNR) considering the cubic metric (CM) [9] that satisfies the target block error rate (BLER) compared to the square 16QAM scheme with a low channel coding rate. Similarly, an efficient modulation scheme with low peak transmission power is necessary for 32QAM and 64QAM schemes. The bit error rate (BER) performance of the star 16QAM scheme and that for the star 32QAM schemes with turbo coding considering non-linearity of the power amplifier (PA) for satellite communications were reported in [10]. Note that star QAM is referred to as amplitude and phase shift keying (APSK) in satellite communications. In this paper, we use the notation of star QAM. In [10], the optimum constellation for the 32APSK scheme was investigated. The optimum constellation for the 64APSK scheme was investigated in [11]. In these papers, the achievable throughput was investigated based on the maximum error-free data rate using mutual information (MI). However, the average BER or BLER performance in a multipath Rayleigh fading channel is not necessarily identical to the results based on MI. This is because the amplitude component is much weaker than the phase component in a multipath Rayleigh fading channel. Hence, we investigated the average BLER performance levels of star 32QAM and 64QAM schemes considering the CM based on a comparison to those of cross 32QAM and square 64QAM schemes, respectively [12].

In general, a one-tap linear filter based on the linear minimum mean-square error (LMMSE) criterion is used in a FDE [4], [5]. In the paper, we refer to the LMMSE based FDE as a feed forward-FDE (FF-FDE). To decrease the residual equalization error of the LMMSE based FF-FDE, a turbo FDE was proposed [13]-[16] that involves frequency domain processing of the turbo equalizer [17]. A turbo FDE comprises a FF-FDE and a decision feedback-FDE (DFB-FDE). The DFB-FDE generates a soft-symbol estimate from the extrinsic probability of the log-likelihood ratio (LLR) at the decoder output and the residual error signal of the FF-FDE in the frequency domain. By subtracting the estimated error signal from the FF-FDE output signal, the

turbo FDE achieves a higher BLER performance level compared to FF-FDE. In [18], the improvement in the average BLER performance of the turbo FDE compared to the FF-FDE was shown particularly for 16QAM and 64QAM assuming ideal channel estimation (CE) for DFT-precoded OFDMA. In the turbo FDE, the estimation accuracy of the channel responses affects the achievable BLER performance level. Hence, iterative decision-directed channel estimation (IDDCE) associated with the turbo FDE was proposed and its performance was investigated for QPSK and square QAM schemes for DFT-precoded OFDMA [19].

This paper presents the average BLER performance of the star 16/64QAM schemes employing a FDE and IDDCE for DFT-precoded OFDMA. By using soft-symbol replicas based on the extrinsic LLR at the Max-Log-MAP (maximum *a posteriori* probability) decoder output and a reference signal (RS), the accuracy of the channel response is improved in the iterative inner loop employing the FF-FDE at an iteration of the outer loop of the turbo FDE. The operational principle of the IDDCE is the same as that in [19]. In general, the soft-symbol estimate for the turbo FDE and IDDCE is generated from the LLR of the extrinsic probability (extrinsic LLR) of each bit at the decoder output. Recently, it was reported in [20] and [21] that for multiple-input multiple-output (MIMO) spatial division multiplexing (SDM), the turbo soft interference canceller (SIC) using a soft-symbol estimate based on the *a posteriori* LLR achieves better BER or BLER performance compared to that with a soft-symbol estimate based on the extrinsic LLR. Hence, we investigate the BLER performance of a turbo FDE with IDDCE using a soft-symbol estimate based on the *a posteriori* LLR or extrinsic LLR. Moreover, we consider a CM, which is an empirical criterion corresponding to the transmission back-off of the transmitter PA [9]. Then, under the best IDDCE conditions, we compare the average BLER performance levels of the star 16/64QAM schemes using the turbo FDE compared to those of the square 16/64QAM in a frequency-selective Rayleigh fading channel. The rest of the paper is organized as follows. First, Section II describes the transmitted signal representation. Section III gives details on the structure of the turbo FDE. Section IV presents the operation of the IDDCE with the selection of soft-symbol estimations. Then, Section V describes the computer simulation evaluation followed by Section VI which gives our concluding remarks.

II. TRANSMITTED SIGNAL REPRESENTATION

Fig. 1 shows the transmitter structure for SC-FDMA using DFT-precoded OFDMA. An information bit stream is channel-encoded using a turbo code with the coding rate of $R = 1/3$ and with the constraint length of 4 bits. The generator polynomials of $R = 1/3$ turbo code are given as $G = [1, g_1/g_0]$ and (g_1/g_0), where $g_0 = [1011]$ and $g_1 = [1101]$. A higher coding rate than $R = 1/3$ is

generated by puncturing the parity bit for the $R = 1/3$ code. The bit-interleaver within the duration of one subframe permutes the coded bits. The coded bit sequence after interleaving is partitioned into L blocks. The coded bits after interleaving are given as $\mathbf{c} = \left[\mathbf{c}_{l,0}^T \cdots \mathbf{c}_{l,k}^T \cdots \mathbf{c}_{l,K-1}^T \right]^T$ ($l = 0,\dots, L$ - 1) in vector notation, which consists of K sets of M code bits $\mathbf{c}_{l,k} = \left[c_{l,k,0} \cdots c_{l,k,M-1} \right]^T$ (the notation of $[\ ]^T$ denotes transposition). Here, the K value corresponds to the number of data-modulated symbols within one FFT block. It also corresponds to the number of subcarriers. In a modulation mapping block, the coded bit is mapped into symbol sequence $x_{l,k} = \mu\left(\mathbf{c}_{l,k} \right)$ among the M-ary constellation to generate a symbol vector with the length of K, $\mathbf{x}_l = \left[x_{l,0} \cdots x_{l,k} \cdots x_{l,K-1} \right]^T$, where $\mathbf{x}_l$ denotes the l-th block of $\mathbf{x}$. The mapping function, μ, performs mapping of code bits according to a 2^M-ary symbol alphabet $S = \left\{ s_0 \cdots s_{2^M-1} \right\}$, where each s_i ($i = 0,\dots, 2^M$-1) corresponds to a binary bit pattern, $\left\{ b_{i,0} \cdots b_{i,M-1} \right\}$, $b_{i,j} \in \{0,1\}$. We assume the 16QAM or 64QAM modulation scheme, i.e., $M = 4$ or 6.
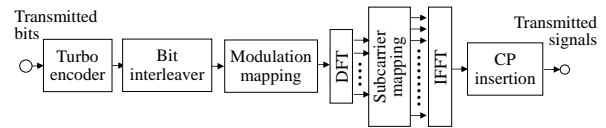

Fig. 1. Transmitter structure.

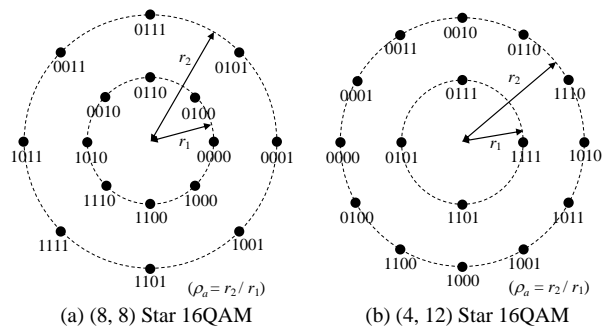
(a) (8, 8) Star 16QAM   (b) (4, 12) Star 16QAM

Fig. 2. Signal constellation of star 16QAM schemes.

Star QAM constellations comprise N concentric rings. In each ring, the PSK points are spaced uniformly. Let (x, y) be the constellation for the star QAM schemes. Then, amplitude $g(j)$ and phase $\phi(j)$ of signal constellation s_i for star QAM are represented as $g(j) = r_v = \sqrt{x^2 + y^2}$ and $\phi(j) = \left(2\pi/n_v \right) j + \theta_v = \tan^{-1}\left(y/x \right)$, respectively. Parameters n_v, r_v, and θ_v are the number of signal points, radius, and relative phase shift for the v-th ring, respectively ($j = 1,\dots, n_v$ in the v-th ring). Fig. 2 shows signal constellations of the (8, 8) and (4, 12) star 16QAM schemes with $N = 2$ rings, which we used in the paper. In Fig. 2, ρ_a indicates the ring ratio of the inner ring amplitude, r_1, to the outer ring amplitude, r_2. For (8, 8) star 16QAM, the amplitude component, $g(j)$, is given as

$g(j) = r\sqrt{8/1+\rho_a^2}$ where r is 1 and ρ_a for the inner and outer rings, respectively. The phase component is given as $\phi(j) \in \{\eta\pi/4\}$, where $\eta = 0, 1, \ldots, 7$. Similarly, for the (4, 12) star 16QAM, the amplitude is given as $g(j) = r\sqrt{16/1+3\rho_a^2}$. The phase component is given as $\phi(j) \in \{\eta\pi/2\kappa\}$, where $\kappa = 1$ and $\eta = 0, 1, 2, 3$ for the inner ring, and $\kappa = 3$ and $\eta = 0, 1, \ldots, 11$ for the outer ring. Moreover, for the star 64QAM schemes, we investigate 2 types of signal constellations, i.e., (8, 24, 32) for $M = 3$ and (16, 16, 16, 16) for $M = 4$. Fig. 3 shows a signal constellation for the (16, 16, 16, 16) star 64QAM scheme. The ring ratios of the (16, 16, 16, 16) star 64QAM scheme are defined as $\rho_a = r_2/r_1$, $\rho_b = r_3/r_1$, and $\rho_c = r_4/r_1$.
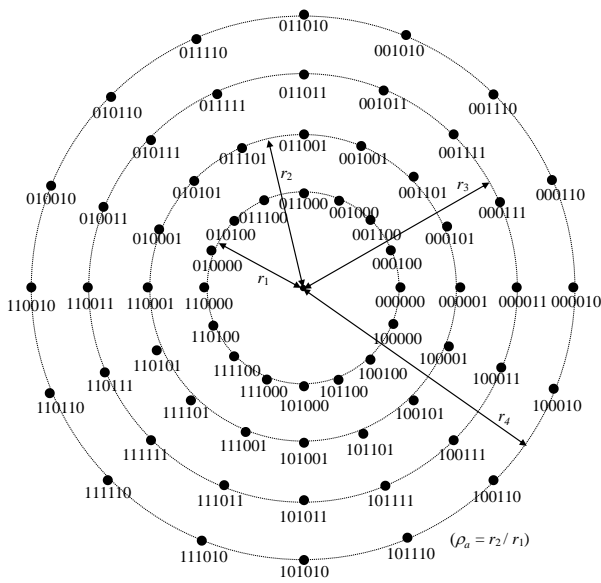

Fig. 3. Signal constellation of (16, 16, 16, 16) star 64QAM schemes.

Data-modulated symbol $x_{l,k}$ is mapped into the t-th FFT block ($t = 1,\ldots,14, t \neq 4,11$) as $x_{t,k}$. Note that the modulation phase is known at the receiver for the RS symbols for $t = 4$ and 11. The data-modulated symbol sequence in the t-th FFT block is converted by the K-point DFT, $\mathbf{F}_K$, into a frequency domain signal with K components (subcarriers), $\mathbf{X}_t = \mathbf{F}_K \mathbf{x}_t$, where $\mathbf{X}_t = [X_{t,0} \cdots X_{t,k} \cdots X_{t,K-1}]^T$ (we use a subcarrier index that is the same as the symbol index in a FFT block for simplicity). In the computer simulation evaluation in Section V, we set $K = 60$, i.e., the transmission bandwidth is $B_{Tx} = 5$ RBs (900 kHz). In the subcarrier mapping part, the symbol vector, $\mathbf{X}_t$, is mapped into the assigned transmission bandwidth. The operation of the subcarrier mapping is expressed as an N_{FFT} x K matrix, $\mathbf{Q}_{N_{FFT} \times K} (N_{FFT} \geq K)$, where N_{FFT} denotes the number of points for the following inverse FFT (IFFT). Matrix $\mathbf{Q}_{N_{FFT} \times K}$ is given as $\mathbf{Q}_{N_{FFT} \times K} = (\mathbf{0}_{z \times K} \quad \mathbf{I}_K \quad \mathbf{0}_{(N_{FFT}-z-K) \times K})^T$, where z ($z \in \{0,1,\ldots(N_{FFT}-K-1)\}$) represents the subcarrier position in which the 0-th subcarrier of the K-subcarrier

signal is assigned and $\mathbf{I}_K$ denotes the K x K identity matrix. Parameter N_{FFT} is set to 1024. After padding (N_{FFT} - K) zeros, the IFFT converts the frequency-domain signal into a time-domain signal as $\mathbf{s}_t = \mathbf{F}_{N_{FFT}}^{-1} \mathbf{Q}_{N_{FFT} \times K} \mathbf{X}_t$. Here, $\mathbf{F}_{N_{FFT}}^{-1}$ indicates the IFFT matrix. Finally, a CP is appended to each FFT block to avoid inter-block interference.

III. TURBO FDE

Fig. 4 shows the receiver structure including a turbo FDE and IDDCE. At the receiver, two-branch antenna diversity reception is assumed. We assume ideal FFT timing detection. Let $\mathbf{r}_m = [r_m(0), \cdots, r_m(N_{FFT}-1)]^T$ be the received signal block within a subframe at the m-th receiver branch ($m = 1, 2$). It is given in matrix notation as

$$\mathbf{r}_m = \mathbf{h}_m \mathbf{s} + \mathbf{n}_m = \sqrt{\frac{2E_s}{T_s}} \mathbf{h}_m \mathbf{d} + \mathbf{n}_m \qquad (1)$$

where $\mathbf{s}$ is the transmitted signal vector, $\mathbf{d}$ is the transmitted symbol vector, $\mathbf{n}_m$ is the noise vector comprising an element with zero mean and the variance of σ^2, and $\mathbf{h}_m$ is the circulant matrix of the channel impulse response with the size of $N_{FFT} \times N_{FFT}$. The received signal block is transformed into frequency domain signal vector $\mathbf{R}_m = [R_m(0), \cdots, R_m(N_{FFT}-1)]^T$ by the FFT and is expressed as

$$\mathbf{R}_m = \mathbf{F}\mathbf{r}_m = \sqrt{\frac{2E_s}{T_s}} \mathbf{H}_m \mathbf{D} + \mathbf{N}_m \qquad (2)$$

where $\mathbf{H}_m = \mathbf{F}\mathbf{h}_m \mathbf{F}^H$ is the channel matrix in the frequency domain, $\mathbf{D} = \mathbf{F}\mathbf{d}$ is the frequency domain signal vector, $\mathbf{N}_m = \mathbf{F}\mathbf{n}_m$ is the frequency domain noise vector, $\mathbf{F}$ is the FFT matrix with the size $N_{FFT} \times N_{FFT}$, and $(\ )^H$ denotes the Hermitian transpose operation. The u-th frequency component, $R_m(u)$, of $\mathbf{R}_m$ at the m-th receiver branch is given as

$$R_m(u) = \sqrt{\frac{2E_s}{T_s}} H_m(u)D(u) + N_m(u) \qquad (3)$$

where $H_m(u) = \sum_{l=0}^{L-1} h_{l,m} \exp(-j2\pi u\tau_l/N_{FFT})$, $D(u) = 1/\sqrt{N_{FFT}} \sum_{t=0}^{N_{FFT}-1} d(t)\exp(-j2\pi ut/N_{FFT})$, and $N_m(u) = 1/\sqrt{N_{FFT}} \sum_{t=0}^{N_{FFT}-1} n_m(t)\exp(-j2\pi ut/N_{FFT})$. In addition, $h_{p,m}$ and τ_p represent the channel impulse response for the p-th path at the m-th receiver branch and the delay for the p-th path, respectively. Then, we obtain k subcarriers including the desired signal from u samples by removing ($N_{FFT} - K$) subcarriers in the frequency domain.
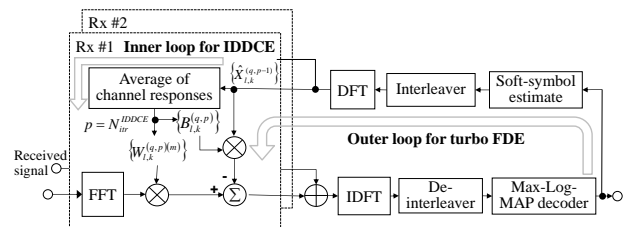

Fig. 4. Receiver structure including turbo FDE and IDDCE.

Let $\overline{H}_k^{(q)(m)}$ be the estimated channel response at the k-th subcarrier after de-mapping in a subframe at the m-th receiver branch for the q-th iteration of the turbo FDE ($1 \le q \le N_{itr}^{TFDE}$). Then, the LMMSE based FF-FDE weight is given as [18], [22]

$$W_k^{(q)(m)} = \left(1 - \left(\rho^{(q-1)}\right)^2\right)\overline{H}_k^{(q)(m)*} \Big/ \left[\sigma^2 + \left(1 - \left(\rho^{(q-1)}\right)^2\right)\sum_{m'=0}^{1}\left|\overline{H}_k^{(q)(m')}\right|^2\right]\gamma^{(q)} \quad (4)$$

In (4), received SNR $\gamma^{(q)}$ is given as

$$\gamma^{(q)} = \left(1/12xK\right)\sum_{m=1}^{2}\sum_{u=k}^{12xK}W_k^{(q)(m)}\overline{H}_k^{(m)} \quad (5)$$

Moreover, $\rho^{(q)}$ is the error correlation of the decoded bit in the previous iteration loop and is defined as $\rho^{(q)} = E\left[\hat{x}_{l,k}^{(q)}x_{l,k}^*\right]\Big/E\left[\left|x_{l,k}\right|^2\right]$ [23]. At the initial iteration of the turbo FDE, the FF-FDE weight is given as $W_k^{(1)(m)} = \overline{H}_k^{(1)(m)*}\Big/\left(\sum_{m'=0}^{1}\left|\overline{H}_k^{(1)(m')}\right|^2 + \sigma^2\right)$. We assume ideal estimation of the noise power, σ^2, in the denominator of the FF-FDE weight. Then, the k-th subcarrier, $R_{l,k}^{(m)}$, after frequency domain equalization and coherently combining of receiver branches is obtained as

$$\hat{R}_{l,k}^{(q)} = \sum_{m=0}^{1}W_k^{(q)(m)}R_{l,k}^{(m)} = \sqrt{\frac{2E_s}{T_s}}\hat{H}_k^{(q)(m)}D_{l,k} + \hat{N}_k^{(q)(m)} , \quad (6)$$

where $\hat{H}_k^{(q)} = \sum_{m'=0}^{1}W_k^{(q)(m)}\overline{H}_k^{(q)(m)}$ and $\hat{N}_{l,k}^{(q)} = \sum_{m=0}^{1}W_k^{(q)(m)}N_{l,k}^{(m)}$ are the equivalent channel response and noise component after frequency domain equalization. An inverse DFT (IDFT) converts the frequency domain signal after diversity combining into a time domain signal. We compute the squared Euclidean distances between the received symbol and symbol replica candidates that contain bit "0" or "1" at the j-th bit position. Then, we compute the LLR of *a posteriori* probability using the minimum squared Euclidean distance for bits "0" and "1" [24]. Let $\overline{r}_{l,k}^{(q)}$ be the signal of the k-th symbol within a FFT block at the q-th iteration of the turbo FDE. Then, the *a posteriori* LLR when the j-th bit of the k-th symbol, $c_{k,j}$, becomes "0" or "1" is computed as

$$\begin{aligned}\Lambda_{APP}^{(q)}\left(c_{l,k,j}\right) &= \ln\left\{P\left(c_{l,k,j}=0\middle|\overline{r}_{l,k}^{(q)}\right)\Big/P\left(c_{l,k,j}=1\middle|\overline{r}_{l,k}^{(q)}\right)\right\} \\ &= \max_{s_i \in \chi_0^i}\ln\left\{P\left(\hat{x}_{l,k}^{(q)}\middle|c_{l,k,j}=0\right)\right\} - \max_{s_i \in \chi_1^i}\ln\left\{P\left(\hat{x}_{l,k}^{(q)}\middle|c_{l,k,j}=1\right)\right\} \\ &= \max_{s_i \in \chi_0^i}\left\{\frac{-\left(\hat{x}_{l,k}^{(q)}-\left|\tilde{w}^{(q)}\right|s_i\right)^2}{2\sigma^2\left|\tilde{w}^{(q)}\right|^2}\right\} - \max_{s_i \in \chi_1^i}\left\{\frac{-\left(\hat{x}_{l,k}^{(q)}-\left|\tilde{w}^{(q)}\right|s_i\right)^2}{2\sigma^2\left|\tilde{w}^{(q)}\right|^2}\right\}\end{aligned} \quad (7)$$

In (7), the equalizer weight, which is used for generating received symbol replicas, is given as $\tilde{w}^{(q)} = 1/K\sum_{l'=0}^{K-1}\hat{w}_{l'}^{(q)}$ and $\chi_{0/1}^j$ denotes a set of symbol constellations containing bit "0" or "1" at the j-th bit position. Here, $\hat{w}_l^{(q)}$ is a channel impulse response after diversity combining and is multiplied by the LMMSE based equalizer weight, which is given as

$$\hat{w}_l^{(q)} = IDFT\left\{\sum_{m=0}^{1}\overline{H}_k^{(q)(m)}W_k^{(q)(m)}\right\} \quad (8)$$

After deinterleaving, the *a posteriori* LLR, $\Lambda_{APP}^{(q)}\left(\mathbf{c}_{l,k}\right)$, is fed into the Max-Log-MAP decoder [25] as *a priori* information. The Max-Log-MAP decoder computes the *a posteriori* LLR of the code bits. The estimates of the code bits, $\Lambda_{APP}^{(q)}\left(\mathbf{c}_{l,k}\right)$, are feedback to generate soft-symbol estimates for the turbo FDE and IDDCE.

The extrinsic LLR at the Max-Log-MAP decoder output, $\Lambda_{EXT}^{(q)}\left(\mathbf{c}_{l,k}\right) = \Lambda_{APP}^{(q)C}\left(\mathbf{c}_{l,k}\right) - \Lambda_a^{(q)}\left(\mathbf{c}_{l,k}\right)$, is generated by eliminating the input signal, i.e., *a priori* LLR $\Lambda_a^{(q)}\left(\mathbf{c}_{l,k}\right)$, from the output signal of the Max-Log-MAP decoder. The extrinsic LLR value is represented as $\Lambda_{EXT}^{(q)}\left(c_{l,k,j}\right) = \ln\left[\left(x_{l,k}\middle|c_{l,k,j}=0\right)\Big/P\left(x_{l,k}\middle|c_{l,k,j}=1\right)\right]$. Let $\lambda\left(c_{l,k,j}\right)$ be the LLR for the j-th bit of the k-th symbol, and the probabilities that bit $c_{l,k,j}$ is equal to 0 and 1 are given as $P\left(c_{l,k,j}=0\right) = \frac{\exp\left[\lambda\left(c_{l,k,j}\right)\right]}{1+\exp\left[\lambda\left(c_{l,k,j}\right)\right]}$ and $P\left(c_{l,k,j}=1\right) = \frac{\exp\left[-\lambda\left(c_{l,k,j}\right)\right]}{1+\exp\left[-\lambda\left(c_{l,k,j}\right)\right]}$, respectively. Hence, the expectation and variance of a symbol, $\mathbf{x}_{l,k} = \mu\left(c_{l,k,0}\cdots c_{l,k,M-1}\right)$, are given using a 2^M-ary symbol alphabet as

$$E\left\{x_{l,k}\right\} = \sum_{s_i \in A}s_i P\left(x_{l,k}=s_i\right)$$

$$\text{var}\left\{x_{l,k}\right\} = \left(\sum_{s_i \in A}\left|s_i\right|^2 P\left(x_{l,k}=s_i\right)\right) - \left|E\left\{x_{l,k}\right\}\right|^2 \quad (9)$$

Since we assume that the bits within one symbol are independent due to the interleaver, $P\left(x_{l,k}=s_i\right)$ is given as $P\left(x_{l,k}^{(q)}=s_i\right) = \prod_{j=0}^{M-1}P\left(c_j=b_{i,j}\right)$.

The DFT converts time domain sample sequence $\hat{x}_{l,k}^{(q)}$ into frequency domain signal $\hat{X}_{l,k}^{(q)}$. The error correlation error of decoded bit $\rho^{(q)}$ is computed from the extrinsic LLR at the Max-Log-MAP decoder output. In the second iteration loop or later, the computed residual equalizer error signal is subtracted from the FF-FDE output signal. The DFB-FDE weight, $B_{l,k}^{(q)}$, of the k-th subcarrier at the q-th iteration is given as [18], [22]

$$B_{l,k}^{(q)} = \left(\sum_{m=0}^{1}W_k^{(q)(m)}\overline{H}_k^{(q)(m)} - \gamma^{(q)}\right)\rho^{(q-1)} \quad (10)$$

The resultant turbo FDE output of the m-th receiver branch at the q-th iteration is obtained as

$$\hat{A}_{l,k}^{(q)} = \sum_{m=0}^{1}\left(Y_{l,k}^{(m)}W_k^{(q)(m)}\right) - B_{l,k}^{(q)}\hat{X}_{l,k}^{(q-1)} \quad (11)$$

The output signals of the turbo FDE of the 2 receiver branches are combined coherently. Then, the *a posteriori* LLR of a coded bit of "0" or "1" is computed by using the operation in (7). At the last iteration in the turbo FDE loop, the *a posteriori* LLR is hard-decided to recover the transmitted bits.

IV. IDDCE WITH SELECTION OF SOFT-SYMBOL ESTIMATIONS

Fig. 5 shows the operation of IDDCE for the turbo FDE. At the first iteration of IDDCE in the first iteration

of the turbo FDE, the channel response of each subcarrier position is estimated using only the RS. Let $\widetilde{H}_{t,k}^{(m)}$ be the channel response at the k-th subcarrier of the t-th FFT block at the m-th receiver branch. To reduce the noise component, we coherently average the channel response at the k-th subcarrier over $2F_{avg}+1$ subcarriers with that at the subcarrier of interest as the center. The channel response averaged in the frequency domain, $\widehat{H}_{t,k}^{(m)}$, is given as

$$\widehat{H}_{t,k}^{(m)} = \sum_{f=-F_{avg}}^{F_{avg}} \alpha_f \widetilde{H}_{t,(k+f)}^{(m)} \tag{12}$$

In (12), coherent summation using weighting factor α_f ($\sum_{f=-F_{avg}}^{F_{avg}} \alpha_f = 1$) is employed considering frequency selectivity suffered in a multipath Rayleigh fading channel. In the evaluation, we set $[\alpha_0, \alpha_{+1/-1}, \alpha_{+2/-2}] = [0.33, 0.22, 0.11]$ with $F_{avg} = 2$ for 16QAM and $[\alpha_0, \alpha_{+1/-1}] = [0.5, 0.25]$ with $F_{avg} = 1$ for 64QAM. The computed $\widehat{H}_{t,k}^{(m)}$ is further coherently averaged to $\overline{H}_k^{(m)} = \{(\widehat{H}_{4,k}^{(m)} + \widehat{H}_{11,k}^{(m)})\}/2$ over two RS symbols within the duration of a subframe.
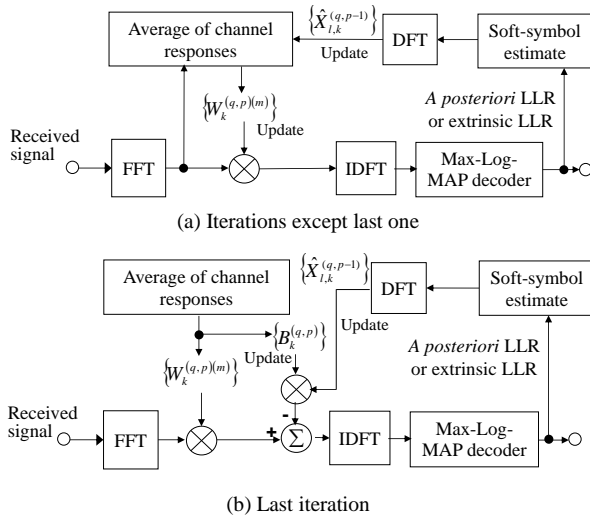

Fig. 5. Operation of IDDCE for turbo FDE.

For an iteration of the turbo FDE, the IDDCE loop is iterated N_{itr}^{IDDCE} times. Let $G_{t,k}^{(q,p)(m)}$ be the channel response at the q-th iteration in the outer loop for the turbo FDE of the p-th iteration in the inner loop for IDDCE ($p = 1,\ldots, N_{itr}^{IDDCE}$). As explained earlier, $\overline{G}_k^{(1,1)(m)} = \overline{H}_k^{(m)}$. Let $\hat{X}_{t,k}^{(q,p)}$ be the soft-symbol replica at the k-th subcarrier of the t-th FFT block in the frequency domain at the combination of the (q, p)-th iteration. Then, the channel response at the k-th subcarrier of the t-th FFT block, $\widetilde{G}_k^{(q,p)(m)}$, is estimated by multiplying the complex conjugate of the soft-symbol estimation, $\hat{X}_{t,k}^{(q,p)}$, to the received signal, $Y_{t,k}^{(m)}$. In the same way as RS based CE, channel response $\widehat{G}_{t,k}^{(q,p)(m)}$ is estimated after weighted coherent averaging in the frequency domain using (12). Except for the case of $(q, p) = (1, 1)$, the channel response at the k-th subcarrier is

averaged coherently over 14 FFT blocks including 2 RS blocks as $\overline{G}_k^{(q,p)(m)} = \sum_{t=1}^{14} \widehat{G}_{t,k}^{(q,p)(m)} / 14$. Since the signal energy of all FFT blocks including the data symbols are used for CE, IDDCE improves the CE accuracy. In IDDCE, only the FF-FDE based on (4) is used to improve the accuracy of the extrinsic LLR at the Max-Log-MAP decoder output when inner loop iteration p is less than N_{itr}^{IDDCE} for an iteration of the outer loop. In the FF-FDE, we replace $\overline{H}_k^{(m)}$ of the FF-FDE weight in (4) with $\overline{G}_k^{(q,p)(m)}$ (error correlation is set to $\rho^{(q,p)} = 0$ when $p < N_{itr}^{IDDCE}$). When $p = N_{itr}^{IDDCE}$ at an iteration of the turbo FDE, both the FF-FDE and DFB-FDE are applied. Based on the results in [19], we set $N_{itr}^{TFDE} = 2$ and $N_{itr}^{IDDCE} = 2$ in the subsequent evaluations.

V. COMPUTER SIMULATION EVALUATION

TABLE I. MAJOR SIMULATION PARAMETERS

Entire transmission bandwidth		10 MHz
UE transmission bandwidth		5 RBs (= 900 kHz)
Number of FFT samples		1024
Subcarrier spacing		15 kHz
Symbol duration	Effective symbol duration	66.7 μs
	Cyclic prefix length	4.7 μs
Subframe length		1 ms (14 FFT blocks)
Data modulation		(4, 12), (8, 8) Star 16QAM, (8, 24, 32), (16, 16, 16, 16) Star 64QAM (as a reference Square 16/64QAM)
Channel coding / Decoding		Turbo code (R = 1/3, 1/2, 2/3, Constraint length is 4 bits) / Max-Log-MAP decoding (8 iterations)
Number of receiver antennas		2
FFT timing detection		Ideal detection
Frequency domain equalizer		Turbo FDE
Channel estimation		IDDCE (RS based CE)
Channel model		ETU channel model ($\tau_{rms} = 0.99 \mu s$)
Maximum Doppler frequency, f_D		5.55 Hz

Table I gives the major computer simulation parameters. We assumed the 9-path Extended Typical Urban (ETU) channel model as the propagation channel model [26]. The root mean square (r.m.s.) delay spread of the ETU channel model is $\tau_{rms} = 0.99 \mu s$ [26]. The fading maximum Doppler frequency is set to $f_D = 5.55$ Hz assuming a pedestrian environment with a low moving speed. We investigate the BLER performance level from the required average BLER considering the CM. The CM is defined in the equation below [9].

$$\mathrm{CM} = \frac{20\log_{10}(\xi_{rms}) - 1.52}{1.56} \tag{13}$$

where ξ_{rms} represents the r.m.s. value of the instantaneous cubic amplitude for each symbol that is normalized by the average amplitude of the input signal. In (13), "1.52" and "1.56" are empirical factors based on the performance of an actual PA.

Table II and Table III give the computed CM values for the star 16QAM and 64QAM schemes with the minimum ring ratio, ρ_a, as a parameter, respectively. We see from Table II that the star 16QAM schemes achieve lower CM values compared to those for square 16QAM

when ρ_a is small. This is because there are fewer transitions that cross the origin for star 16QAM than for square 16QAM. From Table III, the CM value of the star 64QAM scheme becomes higher according to the increase in the *N* value. However, the star 64QAM schemes yield lower CM values compared to that for the square 64QAM for low ring ratios.

TABLE II. COMPUTED CM VALUES FOR VARIOUS 16QAM SCHEMES

| Ring ratio	Cubic metric (dB)		
ρ_a	(4, 12) Star 16QAM	(8, 8) Star 16QAM	Square 16QAM
1.2	1.28	1.32	
1.5	1.45	1.68	
1.8	1.59	2.04	2.13
2.0	1.66	2.24	
2.5	1.79	2.60	
3.0	1.86	2.84	

TABLE III. COMPUTED CM VALUES FOR VARIOUS 64QAM SCHEMES

| Ring ratio	Cubic metric (dB)	Ring ratio	Cubic metric (dB)	
ρ_a, ρ_b	(8, 24, 32) Star 64QAM	ρ_a, ρ_b, ρ_c	(16, 16, 16, 16) Star 64QAM	Square 64QAM
1.2, 1.4	1.36	1.2, 1.4, 1.6	1.58	
1.3, 1.6	1.46	1.3, 1.6, 1.9	1.82	
1.5, 2.0	1.64	1.5, 2.0, 2.5	2.22	
1.8, 2.6	1.83	1.8, 2.6, 3.4	2.60	
2.0, 3.0	1.92	2.0, 3.0, 4.0	2.77	2.33
2.5, 4.0	2.07	2.5, 4.0, 5.5	3.03	
3.0, 5.0	2.16	3.0, 5.0, 7.0	3.17	
3.5, 6.0	2.23	3.5, 6.0, 8.5	3.26	
4.0, 7.0	2.27	4.0, 7.0, 10.0	3.32	

We first investigate the best ring ratio of the star 16/64QAM schemes using the turbo FDE from the viewpoint of the required average received SNR satisfying the target average BLER assuming ideal CE. Figs. 6(a) and 6(b) show the required average received SNR at the average BLER of 10^{-2} considering the CM of the star 16QAM and 64QAM schemes, respectively, using the turbo FDE as a function of ring ratio ρ_a. In [27], members of our research group showed that the BLER improves most when the difference in the radius between the contiguous rings is almost identical. Hence, we parameterize the minimum ring ratio ρ_a when the number of rings is greater than 2. In Fig. 6(a) and Fig. 6(b), the performance levels using FF-FDE based on the LMMSE algorithm are represented as dotted lines. The coding rate of the turbo code is parameterized.

Fig. 6(a) shows the required average received SNR considering the CM of the (8, 8) and (4, 12) star 16QAM schemes. We find that the turbo FDE decreases the required average received SNR considering the CM by approximately 0.3 - 0.5 dB compared to the FF-FDE for both the (8, 8) and (4, 12) star 16QAM schemes regardless of the *R* value. Then, we focus on the comparison between the (8, 8) and (4, 12) star 16QAM schemes using the turbo FDE. The figure shows that the

required average received SNR considering the CM is minimized when the ρ_a value is 1.2, 1.5, and 1.8 for *R* = 1/3, 1/2, and 2/3, respectively, for the (8, 8) star 16QAM scheme. Similarly, the best ρ_a value is 1.5, 2.5, and 3.0 for *R* = 1/3, 1/2, and 2/3, respectively, for the (4, 12) star 16QAM scheme. When the ρ_a value is small, the (8, 8) star 16QAM decreases the required average received SNR considering the CM compared to the (4, 12) star 16QAM scheme. In the (8, 8) star 16QAM scheme, independent bit mapping is achieved: three of four bits represent the phase modulation and the remaining one bit represents the amplitude modulation. Hence, the ρ_a value is optimized only from the BLER of the one bit representing the amplitude component. The decoding error in the amplitude component is mitigated by the high coding gain when using a low coding rate such as *R* = 1/3. The resultant low ring ratio brings about a reduction in the CM value. Fig. 6(a) also shows that the (8, 8) star 16QAM scheme decreases the required average received SNR considering the CM with the best ρ_a value compared to the (4, 12) star 16QAM scheme for *R* = 1/3 and 1/2.
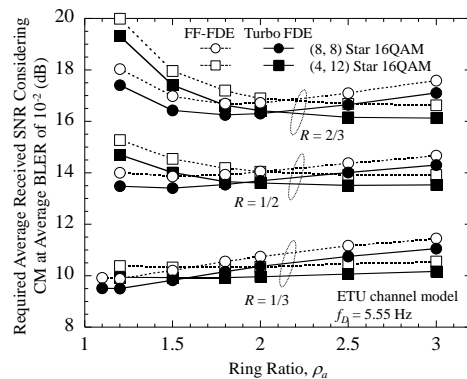
(a) 16QAM
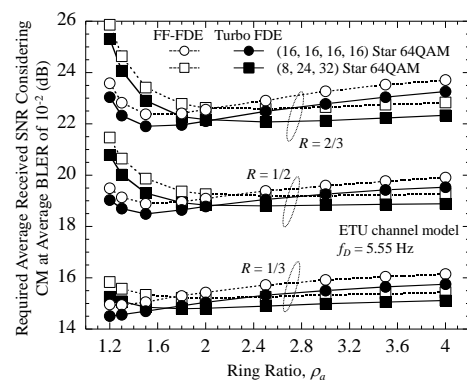
(b) 64QAM

Fig. 6. Required average received SNR considering CM at the average BLER of 10^{-2} as a function of ring ratio, ρ_a.

Fig. 6(b) shows the required average received SNR at the average BLER of 10^{-2} considering the CM of the (8, 24, 32) and (16, 16, 16, 16) star 64QAM schemes. From the figure, the required average received SNR considering the CM using the turbo FDE is decreased by approximately 0.3 - 0.4 dB compared to that for the FF-

FDE for both star 64QAM schemes irrespective of the *R* value. The required average received SNR considering the CM is minimized when the ρ_a value is 1.8, 2.5, and 2.5 for $R = 1/3$, 1/2, and 2/3, respectively, for the (8, 24, 32) star 64QAM scheme. Similarly, the best ρ_a value is 1.2, 1.2, and 1.5 for $R = 1/3$, 1/2, and 2/3, respectively, for the (16, 16, 16, 16) star 64QAM scheme. Fig. 6(b) clearly shows that the (16, 16, 16, 16) star 64QAM scheme decreases the required average received SNR considering the CM compared to the (8, 24, 32) star 64QAM scheme for a low turbo coding rate such as $R = 1/3$ and 1/2.

Fig. 7 shows the average BLER performance using the turbo FDE associated with IDDCE as a function of the average received SNR per receiver antenna considering the CM. The average BLER performance levels using a soft-symbol estimate based on the *a posteriori* LLR and extrinsic LLR are given for both the RS based CE and ideal CE. In Fig. 6, we plot the average BLER performance of the (8, 8) star 16QAM and that of the (16, 16, 16, 16) star 64QAM. Fig. 7 does not show a distinct BLER difference using the turbo FDE with IDDCE based on the *a posteriori* LLR and extrinsic LLR in the case of ideal CE. Meanwhile, the required average received SNR at the average BLER of 10^{-2} using the turbo FDE with the IDDCE based on the *a posteriori* LLR is decreased by approximately 0.2 dB compared to that based on the extrinsic LLR.
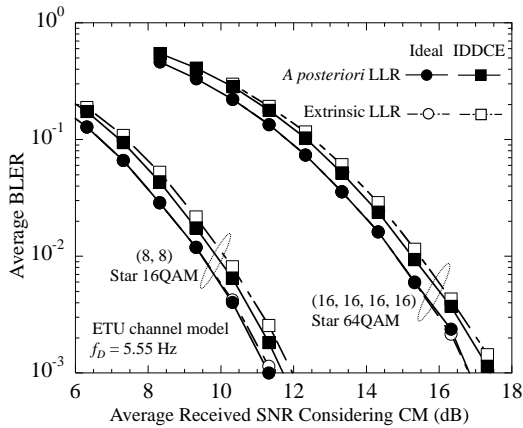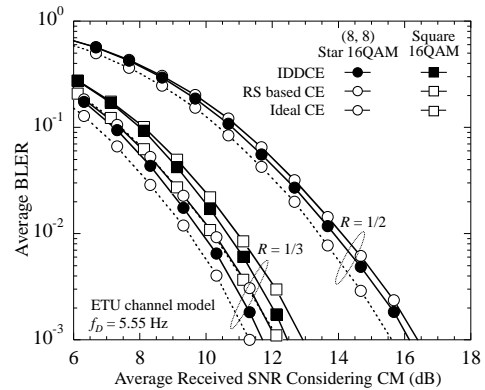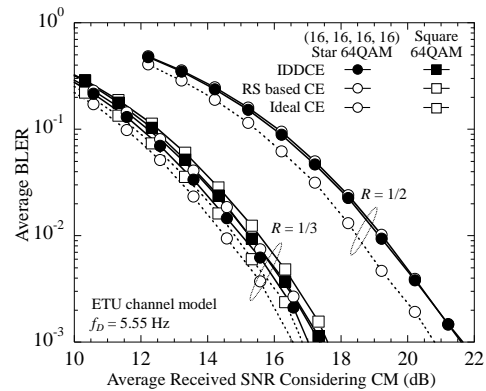

Fig. 7. Average BLER performance using IDDCE with turbo FDE as a function of average received SNR considering CM.

Fig. 8(a) and Fig. 8(b) show the average BLER performance of the 16QAM and 64QAM schemes, respectively, using the turbo FDE associated with IDDCE as a function of the average received SNR per receiver antenna considering the CM. The average BLER performance with the RS based CE and that assuming ideal CE are also plotted for comparison. Fig. 8(a) shows the average BLER performance of the (8, 8) star 16QAM. The performance of the square 16QAM is given only for $R = 1/3$. The figure shows that the loss in the required average received SNR at the average BLER of 10^{-2} considering the CM of the IDDCE from ideal CE is suppressed to approximately 0.4 dB for $R = 1/3$ and 1/2.

Focusing on the performance using the turbo FDE with IDDCE, the required average received SNR considering the CM of the (8, 8) star 16QAM is decreased by approximately 0.8 dB compared to that for the square 16QAM.

(a) 16QAM

(b) 64QAM

Fig. 8. Average BLER performance using IDDCE with turbo FDE as a function of average received SNR considering CM.

Fig. 8(b) shows the average BLER performance of the (16, 16, 16, 16) star 64QAM scheme and that of the square 64QAM. For $R = 1/3$, the required average received SNR at the average BLER of 10^{-2} considering the CM of the (16, 16, 16, 16) star 64QAM is decreased by approximately 0.3 dB compared to that for the square 64QAM scheme when using the turbo FDE associated with IDDCE. However, the improvement from IDDCE compared to that from the RS based CE is slight for $R = 1/2$. Based on the simulation results, we showed that IDDCE is effective in decreasing the required average received SNR for the turbo FDE for star 16/64QAM schemes.

VI. CONCLUSION

This paper presented the average BLER performance of star 16/64QAM schemes employing the IDDCE associated with the turbo FDE for DFT-precoded OFDMA. Computer simulation results showed the best ring ratios of the star 16/64QAM schemes when using the turbo FDE from the viewpoint of the required average

received SNR at the average BLER of 10^{-2} considering the CM. We also showed that the required average received SNR at the average BLER of 10^{-2} using the turbo FDE with the IDDCE based on the *a posteriori* LLR is decreased by approximately 0.2 dB compared to that based on the extrinsic LLR. Then, we showed that the turbo FDE decreased the required average received SNR at the average BLER of 10^{-2} considering the CM by approximately 0.3 - 0.5 dB compared to the LMMSE based FF-FDE for both star 16/64QAM schemes irrespective of the turbo coding rate. Moreover, we showed that the (8, 8) star 16QAM and (16, 16, 16, 16) star 64QAM scheme decreased the required average received SNR considering the CM by approximately 0.8 and 0.3 dB compared to the square 16QAM and 64QAM schemes, respectively, with a low turbo coding rate such as $R = 1/3$ when using turbo FDE associated with IDDCE.

REFERENCES

[1] 3GPP TS36.211 (V9.1.0), "Physical channels and modulation," March 2010.

[2] D. Galda and H. Rohling, "A low complexity transmitter structure for OFDM-FDMA uplink system," in *Proc. IEEE VTC2002-Spring*, vol. 4, May 2002.

[3] R. Dinis, D. Falconer, C. T. Lam, and M. Sabbaghian, "A multiple access scheme for the uplink of broadband wireless access," in *Proc. IEEE Globecom*, vol. 6, Dec. 2004.

[4] H. Sari, G. Karam, and I. Jeanclaude, "Frequency-domain equalization of mobile radio and terrestrial broadcast channels," in *Proc. IEEE Global Telecommunications Conference*, vol. 1, Nov–Dec 1994.

[5] D. Falconer, S. L. Ariyavisitakul, A. B.-Seeyar, and B. Eidson, "Frequency domain equalization for single-carrier broadband wireless systems," *IEEE Commun., Mag.*, vol. 40, April 2002.

[6] J. G. Proakis, *Digital Communications*, 4th ed., New York: McGraw-Hill, 2001.

[7] W. T. Webb, L. Hanzo, and R. Steele, "Bandwidth efficient QAM schemes for Rayleigh fading channels," *IEEE Proc. I*., vol. 138, pp. 169–175, June 1991.

[8] T. Kawamura, Y. Kishiyama, K. Higuchi, and M. Sawahashi, "Comparisons of 16QAM modulation schemes considering PAPR for single-carrier FDMA radio access in Evolved UTRA uplink," in *Proc. IEEE ISSSTA*, Aug. 2006, pp. 332 - 336.

[9] 3GPP, R4-040367, Motorola, "Comparison of PAR and cubic metric for power de-rating," May 2004.

[10] R. D. Gaudenzi, A. G. Fabregas, and A. Martinez, "Performance analysis of turbo-coded APSK modulation over non-linear satellite channels," *IEEE Trans. on Wireless Commun.*, vol. 5, pp. 2396–2407, Sep 2006.

[11] K. P. Liolis and N. S. Alagha, "On 64-APSK constellation design optimization," in *Proc. 10th International Workshop on Signal Processing for Space Communications*, SPSC 2008.

[12] C. Mori, T. Kawamura, N. Miki, and M. Sawahashi, "Link-level performance of Star 32/64QAM schemes using frequency domain equalizer for DFT-precoded OFDMA," in *Proc. WPMC 2012*, Sept 2012.

[13] N. Benvenuto and S. Tomasin, "Block iterative DFE for single carrier modulation," *IEE Electronic Letters*, vol. 38, no. 19, pp. 1144 – 1145, Sept 2002.

[14] G. Huang, A. Nix, and S. Armour, "Decision feedback equalization in SC-FDMA," in *Proc. IEEE PIMRC*, 2008, pp. 1-5.

[15] B. Ng, Chan-Tong Lam, and D. Falconer, "Turbo frequency domain equalization for single-carrier broadband wireless systems," *IEEE Trans. on Wireless Commun.*, vol. 6, no. 2, pp. 759-767, Feb 2007.

[16] M. Sabbaghian and D. Falconer, "Comparison between convolutional and LDPC code-based turbo frequency domain equalization," in *Proc. IEEE Int. Conf. Commun.*, vol. 12, June 2006, pp. 5432-5437.

[17] R. Koetter, A. C. Singer, and M. Tuchler, "Turbo equalization," *IEEE Signal Processing Magazine*, pp. 67- 80, Jan 2004.

[18] G. Berardinelli, B. E. Priyanto, T. B. Sorensen, and P. Mogensen, "Improving SC-FDMA performance by turbo equalization in UTRA LTE uplink," in *Proc. IEEE VTC-Spring*, May 2008, pp. 2557-2561.

[19] C. Mori and Y. Tanaka, T. Kawamura, N. Miki, and M. Sawahashi, "Performance of turbo frequency domain equalizer using iterative decision-directed channel estimation for DFT-precoded OFDMA," in *Proc. WPMC*, June 2013.

[20] M. Witzke, S. Baro, F. Schreckenbach, and J. Hagenauer, "Iterative detection of MIMO signals with linear detectors," in *Proc. IEEE Globecom,* Dec 2003.

[21] B. Ning, R. Visoz, and A. O. Berthet, "Extrinsic versus a posteriori probability based iterative LMMSE-IC algorithms for coded MIMO communications: Performance and analysis," in *Proc. ISWCS,* Aug 2012.

[22] M. M. da Silva, R. Dinis, and A. M. C. Correia, "Iterative frequency-domain receivers for STBC schemes," in *Proc. IEEE VTC2009-Fall*, Oct 2009.

[23] A. Gusmão, P. Torres, R. Dinis, and N. Esteves, "A class of iterative FDE techniques for reduced-CP SC-based block transmission," in *Proc. Int. Symposium on Turbo Codes*, April 2006.

[24] A. Stefanov and T. Duman, "Turbo coded modulation for wireless communications with antenna diversity," in *Proc. IEEE VTC'99*, Sept 1999, pp. 1565-1569.

[25] P. Robertson, E. Villebrun, and P. Hoeher, "A comparison of optimal and sub-optimal MAP decoding algorithms operating in the log domain," in *Proc. IEEE ICC'95*, vol. 2, June 1995, pp. 1009-1013.

[26] 3GPP TS 36.104 (V10.0.0), Sept. 2010.

[27] R. Kobayashi, T. Kawamura, N. Miki, and M. Sawahashi, "Throughput comparisons of 32/64APSK schemes based on mutual information considering cubic metric," *IEICE Trans. on Commun.*, vol. E95-B, no. 12, pp. 3719 – 3727, Dec 2012.

Chihiro Mori received her B.E. degree from Musashi Institute of Technology, Japan in 2012. In 2012, she joined a graduate school of Tokyo City University. In the university, she is engaged in research for star QAM schemes with turbo FDE.

Teruo Kawamura received his B.E. and M.E. degrees from Hokkaido University, Sapporo, Japan in 1999 and 2001, respectively. In 2001, he joined NTT DOCOMO, INC. Since joining NTT DOCOMO, he has been engaged in the research and development of chip equalizer for HSDPA, radio interface of uplink data and control channels for LTE and LTE-Advanced, and experimental evaluations for LTE and LTE-Advanced.

Nobuhiko Miki received his B.E. and M.E. degrees from Kyoto University, Kyoto, Japan in 1996 and 1998, respectively, and received his Dr. Eng. degree from Keio University, Yokohama, Japan in 2009. In 1998, he joined NTT Mobile Communications Network, Inc. (now NTT DOCOMO, INC.) From April 2013, He assumed the position of the Associate Professor of the Department of Electronics and Information Engineering, Faculty of Engineering, Kagawa University. His research interests include mobile communication systems.

Mamoru Sawahashi received his B.S. and M.S. degrees from The University of Tokyo in 1983 and 1985, respectively, and received his Dr. Eng. Degree from the Nara Institute of Technology in 1998. In 1985, he joined the NTT Electrical Communications Laboratories, and in 1992 he transferred to NTT Mobile Communications Network, Inc. (now NTT

DOCOMO, INC.). In NTT, he was engaged in the research of modulation/demodulation techniques for mobile radio. He was also engaged in the research and development of radio access technologies for W-CDMA mobile communications and broadband packet radio access technologies for 3G long-term evolution and for the systems beyond IMT-2000 in NTT DOCOMO. From April 2006, he assumed the position of Professor of the Department of Electronics and Communication Engineering, Musashi Institute of Technology (now Tokyo City University). From 2007 to 2009, he was a part-time director of the Radio Access Development Department of NTT DOCOMO. In 2005, 2006 and 2011, he served as a guest editor of the IEEE JSAC on Intelligent Services and Applications in Next-generation Networks, 4G Wireless Systems, and Advances in Multicarrier CDMA, and Distributed Broadband Wireless Communications.